Iranian Polymer Journal (2022) 31:983–990
https://doi.org/10.1007/s13726-022-01050-y

ORIGINAL RESEARCH

Acrylamide-*ran*-methyl methacrylate copolymers synthesized by copper(0)-catalyzed living radical polymerization

Xi Zhao[1] · Enxiang Liang[1] · Feixiang Zhou[1] · Guoxiang Wang[1] · Yixue Xu[1] · Wenyuan Xu[1]

Received: 14 August 2021 / Accepted: 5 February 2022 / Published online: 29 March 2022

Abstract

A series of well-defined acrylamide/methyl methacrylate random copolymers (PAM-*ran*-PMMA) were synthesized in this work. The polymerization reactions were carried out in *N*,*N*-dimethylformamide (DMF) at 25 °C using Cu(0)/hexamethylenetetramine (HMTA) and CCl_4/hydrazine as the catalyst system and the initiator system, respectively. The number average molecular weights (M_n) and the distribution of molecular weight (M_w/M_n) of copolymers were analyzed by gel permeation chromatography (GPC). Experimental results revealed that the copolymerization reaction follows a pseudo first-order kinetic model. M_n of PAM-*ran*-PMMA increased linearly with the conversion of monomers while a narrow molecular weight distribution was obtained. By means of Fineman–Ross equation, the reactivity ratios of r_1 (AM) and r_2 (MMA) were calculated to be 0.81 and 3.21, respectively. The results implied that the amount of AM unites in PAM-*ran*-PMMA copolymers increased with the increase of the molar ratios of AM/MMA. The structure and the thermal stability of the resultant PAM-*ran*-PMMA copolymer were characterized by Fourier transform infrared spectroscopy (FTIR), nuclear magnetic resonance spectrometry (^{1}H NMR) and thermogravimetric analysis (TGA). TGA revealed that copolymers with a greater content of AM unit exhibited a higher thermal stability. The obtained PAM-*ran*-PMMA copolymer was used as a macroinitiator to perform Cu(0)-catalyzed chain extension experiment, which led to the increase of Mn and demonstrated the living character of the polymerization. This current approach provided a controlled route for the synthesis of well-defined PAM-*ran*-PMMA.

✉ Guoxiang Wang
wanggxwzl@163.com

✉ Yixue Xu
xuyixue@163.com

✉ Wenyuan Xu
xuwenyuan@163.com

[1] College of Chemistry and Chemical Engineering, Hunan Institute of Science and Technology, Yueyang 414006, Hunan Province, China

Graphical abstract

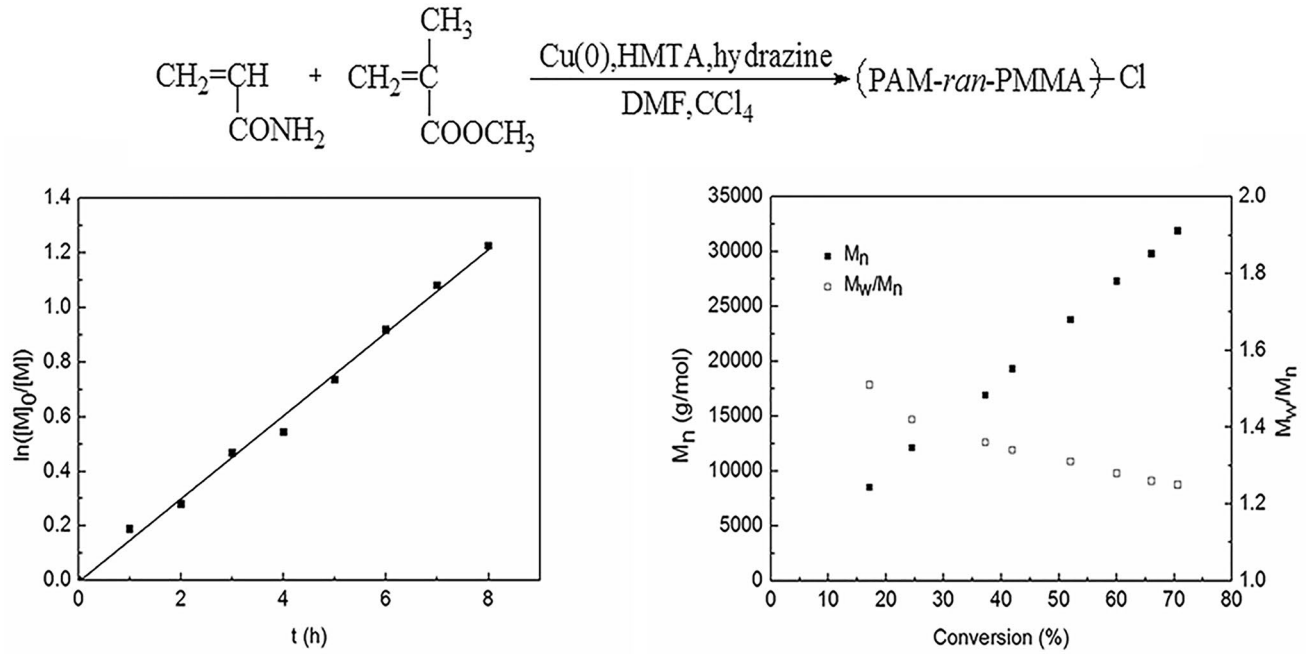

Keywords Cu(0)-catalyzed polymerization · Random copolymers · Controlled radical polymerization · Reactivity ratio · PAM-*ran*-PMMA

Introduction

Controlled radical polymerization (CRP) has become an indispensable method for the synthesis of well-defined polymers with controlled architectures [1–3]. Generally, CRPs are based on the reversible and dynamic equilibrium between dormant species and active species [4]. Despite of the tremendous developments of CRPs in the past decades [5–7], there is not a universal technology for all monomer families. As one of the most robust and versatile technologies of CRPs, atom transfer radical polymerization (ATRP) is suitable for many polymerizable vinyl monomers except for some water-soluble vinyl monomers, such as acrylic acid and acrylamide, due to the complex interaction between Cu(I) species and the monomers [4]. The main disadvantage of ATRP is that the remaining transition metal complex would injure the properties of the resulting materials. This problem could be resolved by the activator regenerated by electron transfer (ARGET) ATRP process, in which the concentration of the catalyst is as low as ppm. During ARGET ATRP process, small amount of catalyst is continuously regenerated by a reducing agent such as tin(II) 2-ethylhexanoate ($Sn(EH)_2$)[5], glucose [6], ascorbic acid [7], β-cyclodextrin (CD) [8], hydrazine [9], or zerovalent metals [10], etc. Additionally, ARGET ATRP can be conducted in the presence of limited amounts of air because ATRP process is started from the oxidatively stable Cu^{II} species as the starting ATRP. The limited amounts of air in the system can be further eliminated during the following reducing/reactivating cycles [11].

Random copolymers are defined as the random distribution of M1 and M2 monomers along the copolymer backbone. Random copolymers usually exhibit better processing and service characteristics than their respective homopolymers [12]. The properties of random copolymers could be flexibly tuned by the adjustment of the relative content of M1 (or M2) in the copolymer chains and the molecular weight as well as the distribution of the molecular weight. Relative to block copolymers, the synthetic procedures of random copolymers are much simplified. Fan et al. [13] have reported that crystallinity of 3-trimethylenecarbonate-*co*-lactide copolymers decreased with the increase of 3-trimethylenecarbonate content. Zhong et al. [14] reported that the component distribution of poly (9,9-dioctylfluorene-*co*-(4,7-dithienyl-benzothiadiazole)) (DOF:DBT = 9:1 mol/mol, PFO-DBT10) random copolymers has remarkable effect on their optoelectronic properties. However, the traditional radical polymerization is limited to control the molecular weight and the molecular weight distribution of random copolymers [15].

Water-soluble polyacrylamide (PAM) polymers are widely used in oil exploitation [16], water pollution treatment [17] and other fields. PAM with controlled structures is a challenge by means of traditional ATRP because of the complexation of amino group and Cu(I) species. This problem could be overcome using Cu(0) as the catalyst. For example, Alsubaie and co-workers [18] have reported the synthesis of PAM polymers with controlled chain lengths and narrow M_w/M_ns through Cu(0)-mediated reversible deactivation radical polymerization of acrylamide monomers. Fan and co-workers [19] have reported Cu(0)-mediated living radical polymerization of acrylamide with waxy potato starch-based macroinitiator. Previous studies have revealed that some properties of water-soluble PAMs could be improved by hydrophobic modification by the incorporation of hydrophobic side chains either at terminal positions or distributed randomly along the backbones [20–22]. Hydrophobic modification would endow PAMs a wide range of applications in industrial products such as paint, adhesives, cosmetics, etc.

Herein, hydrophobic modified PAMs copolymers were synthesized by copolymerization of AM with the commercial hydrophobic vinyl monomer of methyl methacrylate (MMA). A series of acrylamide/methyl methacrylate random copolymers (PAM-*ran*-PMMA) with controlled structures were synthesized by Cu(0)-catalyzed living radical polymerization process. The reactivity ratios of r_1 (AM) and r_2 (MMA) were studied by means of Fineman–Ross equation. To the best of our knowledge, the reports on hydrophobic modified PAMs copolymers with controlled structures are very limited. PAM-*ran*-PMMA copolymers having many polar lateral ester groups and amide groups would exhibit wide applications in industrial fields.

Experimental

Materials

Hydrazine ($N_2H_4{\cdot}H_2O$), Cu(0) power, hexamethylenetetramine (HMTA), *N*,*N*-dimethyllformamide (DMF) and CCl_4 were obtained from Sinopharm Chemical Reagent Co., Ltd. (Shanghai, China) and used without any treatments. MMA was distilled under the reduced pressure prior to use. AM was recrystallized with acetone twice before use.

Cu(0)-catalyzed living radical polymerization kinetics of AM with MMA

Cu(0)-catalyzed living radical polymerization of AM with MMA was conducted at 25 °C in a three-neck flask. The molar ratio of $[AM]_0/[MMA]_0/[CCl_4]_0/[Cu(0)]_0/[HMTA]_0$ was 250:250:1:0.1:0.2. The polymerization reaction was terminated after a given time, and the monomer conversion was analyzed by a gravimetric method. In a typical experiment, AM (710 mg, 0.01 mol), MMA (1 g, 0.01 mol), Cu(0) power (0.3 mg, 0.004 mmol), HMTA (1.1 mg, 0.008 mmol), and 15 mL of DMF containing 2 μL hydrazine hydrate (2.2 M) were charged into the flask. After 30 min of degassing with N_2, the required amounts of CCl_4 (3.9 μL, 0.04 mmol) was added. The flask was sealed, and then transferred to an oil bath at 60 °C. After a period of polymerization, the reaction was terminated. The mixtures were precipitated in a large amount of methanol. The resulting polymers were collected by filtration and dried under vacuum at 25 °C for 24 h.

Cu(0)-catalyzed living radical polymerization of AM with MMA under different monomer concentrations

Under otherwise identical conditions, Cu(0)-catalyzed living radical polymerization of AM with MMA was conducted under higher ratio of [monomer]/[initiator], such as 500 and 400, in which the ratio of $[AM]_0/[MMA]_0$ was 1. After a given polymerization time, the reaction was terminated. The mixtures were precipitated in a large amount of methanol. The resulting polymers were collected by filtration and dried under vacuum at 25 °C for 24 h.

Determination of the reactivity ratios of Cu(0)-catalyzed living radical polymerization of AM with MMA

All polymerizations were conducted with the fixed molar ratio of $[AM]_0/[MMA]_0/[CCl_4]_0/[Cu(0)]_0/[HMTA]_0$, such as 250:250:1:0.1:0.2. The conversion of monomers was less than 10% (by weight), which was determined by gravimetric method. All polymerization reaction times were ranged from 10 ~ 45 min. The content of AM unit was determined by the analysis of N content in the PAM-*ran*-PMMA copolymers with an elemental analyzer.

Characterization

FTIR spectrum was collected by an Avatar 370 T infrared spectrometer (Thermo-Nicolet, USA). Gel permeation chromatography (GPC) was performed on Waters 1515 (Waters, USA) in THF at 35 °C with PMMA as standards. ^{1}H NMR spectrum was recorded on a Bruker 400 MHz with $CDCl_3$ as solvent. Thermal gravimetric analysis (TGA) was conducted on a NETZSH STA409PC instrument (Netzsch, Germany). The flow rate of N_2 was 10 mL/min. The temperature increased from 30 to 800 °C. Elemental analysis (C/H/N) was carried out on a Vario EL Cube (Elementar, Germany).

Results and discussion

Synthesis of PAM-*ran*-PMMA through Cu(0)-catalyzed living radical polymerization process

PAM-*ran*-PMMA copolymers were synthesized in DMF at 25 °C using Cu(0)/hexamethylenetetramine (HMTA), CCl_4, and hydrazine as catalyst system, initiator, and reducing agent, respectively. Figure 1A shows the relationship of the monomer conversion versus the reaction time. The monomer conversion increased with the prolonging of reaction time, and 70% of monomers have been converted within 8 h. $\ln([M]_0/[M])$ versus t is plotted in Fig. 1B. As shown in Fig. 1B, the polymerization reaction presents pseudo first-order kinetics, suggesting that the concentration of growth chain radical is a constant during the polymerization. Figure 1C shows GPC traces of PAM-*ran*-PMMA copolymers. GPC trace shifted towards the high molecular weight region with the increase in reaction time. All GPC traces showed a systematic and unimodal peak. Figure 1D shows the relationship of the monomer conversion with the number average molecular weights and M_w/M_n. The molecular weight of the PAM-*ran*-PMMA with a narrow distribution (M_w/M_n) increased linearly with the increase of monomer conversion. GPC results showed that the reaction was a controlled radical polymerization process under the above reaction conditions.

The FTIR spectrum of PAM-*ran*-PMMA copolymers is depicted in Fig. 2A. The peak at 3400 cm^{-1} corresponded to the O–H stretching vibration of moisture or N–H stretching vibration [23]. The peaks at 2950–3050 cm^{-1} corresponded to the C–H stretching vibration of alkyl chain. The peak at

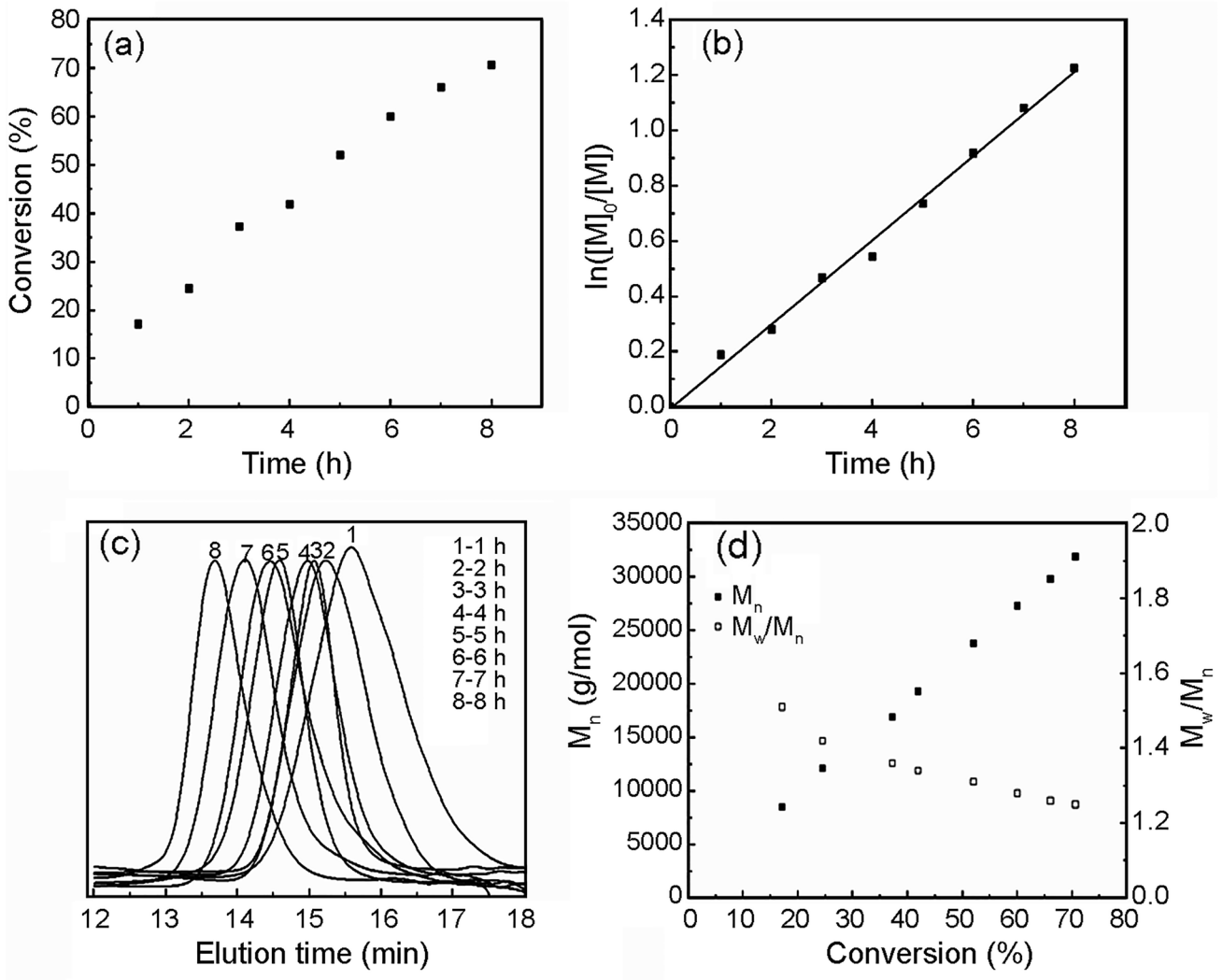

Fig. 1 **A** Monomer conversion versus time plot; **B** relationship between $\ln([M]_0/[M])$ and polymerization time; **C** GPC traces at different times; and **D** the relationship of the number average molecular weight (M_n) and M_w/M_n of the PAM-*ran*-PMMA with the monomer conversion

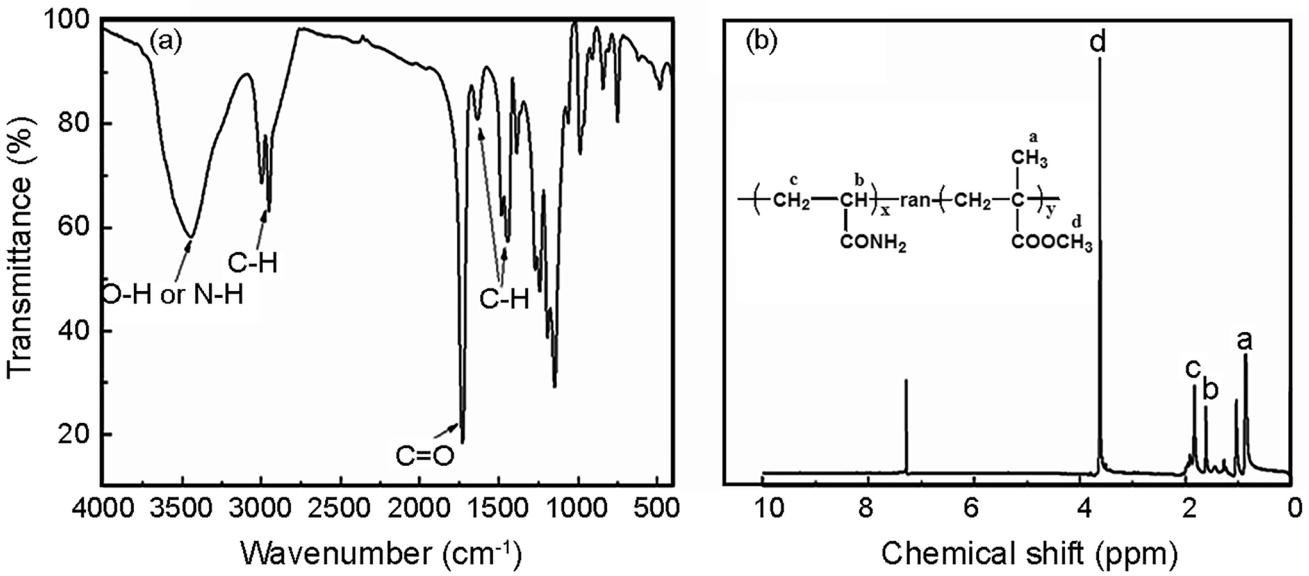

Fig. 2 FTIR (**A**) and ^{1}H NMR (**B**) spectra of PAM-*ran*-PMMA copolymer

Table 1 GPC results of copolymers synthesized under different molar rations of $[AM]_0/[MMA]_0/[CCl_4]_0$

Run	$[AM]_0/[MMA]_0/[CCl_4]_0$	Conversion (%)	$M_{n,GPC}$ (g/mol)	M_w/M_n
1	200:200:1	57.2	24,700	1.29
2	400:400:1	75.1	57,100	1.32
3	500:500:1	80.6	74,600	1.36

The reaction time was 6 h for all cases. $[CCl_4]_0$ was 0.0027 M. The volume of DMF was 15 mL

1730 cm^{-1}, 1632 cm^{-1}, and 1445 cm^{-1} corresponded to the stretching vibrations of C=O and amide groups and deformations of C–H, respectively [24–26]. Typical ^{1}H NMR spectrum of PAM-*ran*-PMMA copolymer is displayed in Fig. 2B. The resonance peaks at $\delta = 0.84$–1.03 ppm, 1.61 ppm, and 1.82 ppm were attributed to the protons of CH_3, CH, and CH_2 group, respectively. The peak at $\delta = 3.60$ ppm corresponded to the protons of $-OCH_3$ group originated from PMMA units.

The effect of the monomer concentration on the polymerization was investigated. Keeping the fixed molar ratio of $[Cu(0)]_0/[HMTA]_0$, such as 1/2, 2 µL hydrazine hydrate was added in 15 mL DMF (2.2 M), and the polymerization was carried out under various molar ratios of $[AM]_0/[MMA]_0/[CCl_4]_0$ ranging from 200/200/1 to 500/500/1. The results are summarized in Table 1. As shown in Table 1, the conversion increased from ~ 57.6% to ~ 80.2% with the change of the molar ratio of $[AM]_0/[MMA]_0/[CCl_4]_0$ from 200/200/1 to 500/500/1within the same polymerization time, revealing the polymerization rate increased with the increase of monomer concentration. Based on GPC analysis, M_ns of copolymers also increased with the increase of the molar ratio of $[AM]_0/[MMA]_0/[CCl_4]_0$ from 200:200:1 to 500:500:1, while a narrow molecular weight distribution ($M_w/M_n < 1.4$) remained, revealing that controllable polymerization reactions could be conducted at a high monomer concentration for the current system. In this study, Cu(0) power was used. Cu(0) can be easily to be oxidized to Cu_2O in production process due to the high surface activation [27]. $N_2H_4{\cdot}H_2O$ can reduce oxide layer (Cu_2O) on the surface of Cu(0) power to Cu(0) [28]. The role of hydrazine is illustrated in Scheme 1.

Investigation of the reactivity ratios

The monomer conversion was less than 10% in all polymerization reactions. The content of PAM in copolymers was analyzed according to the nitrogen element contents, which were determined by elemental analysis. The detailed experimental data are summarized in Table 2. The

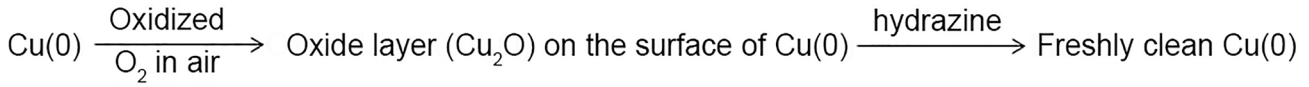

Scheme 1 Illustration of the role of hydrazine

Table 2 Relationship between monomer ratios and copolymer compositions[a]

Run	Conv. (%)	f_1[b]	f_2[c]	F_1[d]	F_2[e]	F[f]	F[g]	f/F^2	$(f-1)/F$	N (% by weight)	C (% by weight)	H (% by weight)	O (% by weight)
1	3.8	0.1	0.9	0.07	0.93	0.11	0.08	17.92	−11.29	1.01	59.55	7.98	31.46
2	7.1	0.3	0.7	0.20	0.80	0.43	0.25	6.77	−2.27	2.95	58.58	7.84	30.63
3	9.4	0.5	0.5	0.32	0.68	1	0.47	4.47	0	4.91	57.69	7.78	29.62
4	7.5	0.7	0.3	0.52	0.48	2.33	1.10	1.93	1.21	8.61	55.95	7.56	27.88
5	4.2	0.9	0.1	0.76	0.24	9	3.10	0.94	2.58	13.4	53.66	7.37	25.57

[a]Copolymerization time was less than 45 min

[b]f_1: the molar fraction of AM in the feed composition

[c]f_2: the molar fraction of MMA in the feed composition

[d]F_1: the molar fraction of AM in the copolymer

[e]F_2: the molar fraction of MMA in the copolymer

[f]$f=f_1/f_2$

[g]$F=F_1/F_2$

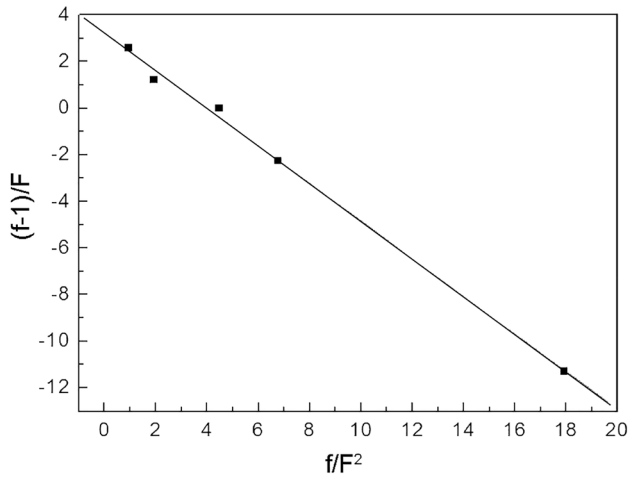

Fig. 3 Plot of $(f-1)/F$ versus f/F^2 for AM and MMA copolymerization

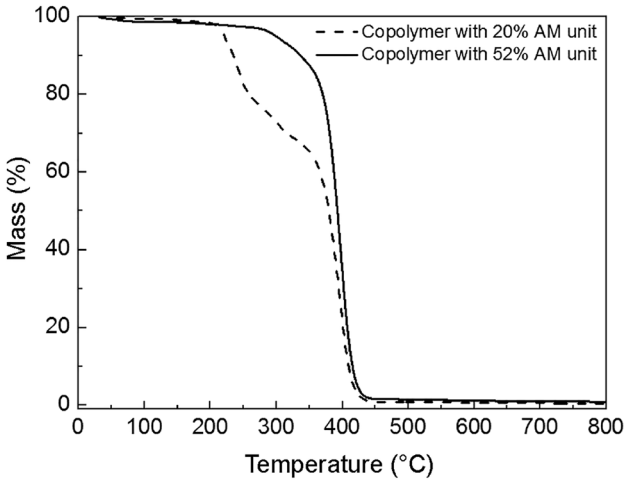

Fig. 4 TGA curves of AM/MMA copolymer with different ratios. PAM-*ran*-PMMA copolymers with ~ 20% (by mol) of AM unit (time 6 h, conversion 71.42%, M_n29600 g/mol, M_w/M_n1.29) and PAM-*ran*-PMMA copolymers with ~ 52% (by mol) of AM unit (time 6 h, conversion 51.72%, M_n26200 g/mol, M_w/M_n1.31)

reactivity ratios of AM and MMA were calculated according to the Fineman–Ross equation [29]:

$$\frac{f-1}{F} = -r_2 \times \frac{f}{F^2} + r_1 \quad (1)$$

where r_1 is the reactivity ratio of AM, r_2 is the reactivity ratio of MMA and f and F are the molar ratios of AM and MMA at the initial stage and the molar ratio of AM and MMA units in the copolymer, respectively.

According to the Fineman–Ross equation, the f/F^2 was used as the abscissa, and the $(f-1)/F$ value was plotted as the ordinate. The linear relationship between $(f-1)/F$ and f/F^2 is observed in Fig. 3. The r_1 and r_2 were calculated to be 0.81 and 3.21 from the intercept and the slope according to Fig. 3, respectively. The r_2 (3.21) was larger than r_1 (0.81), indicating that the probability of AM entering the copolymer chain is smaller than that of MMA. r_1 and r_2 are different from those reported elsewhere. The reported reactivity ratios for copolymerization of AM and MMA at 70 °C in dioxane, dioxane/ethanol mixture and ethanol were 2.45/2.55, 0.82/2.53, 0.44/2.60, respectively [30]. This may be due to different reaction systems.

Thermal stabilities of PAM-*ran*-PMMA copolymers

Figure 4 shows TGA traces of PAM-*ran*-PMMA copolymers with different chemical composites. As shown in Fig. 4, PAM-*ran*-PMMA copolymers with different chemical composites exhibit different thermal weight-loss behaviors. The

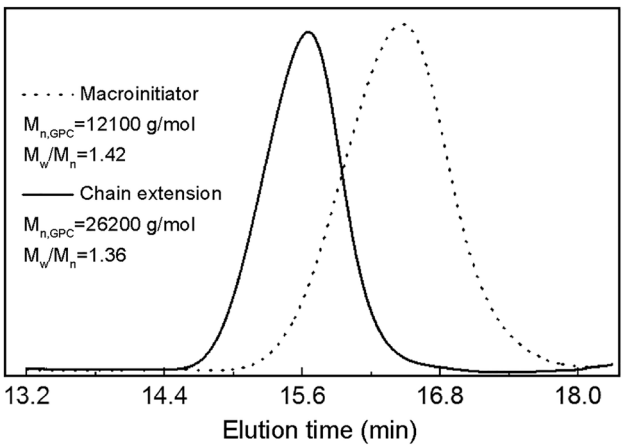

Fig. 5 GPC traces of macroinitiator and block copolymer

starting temperature of thermal decomposition of random copolymers increased with increases in the content of AM unit in copolymers. For example, the starting temperature was about 274 °C for $PAM_{0.52}$-*ran*-$PMMA_{0.48}$ copolymers, whereas it was 212 °C for $PAM_{0.2}$-*ran*-$PMMA_{0.8}$ copolymers. This could be ascribed to increased interchain interactions owing to the increase of PAM content in copolymer chain. Different from $PAM_{0.52}$-*ran*-$PMMA_{0.48}$, there were two weight loss stages in TGA trace of $PAM_{0.2}$-*ran*-$PMMA_{0.8}$. ~ 37% (by weight) weight loss between 212 °C ~ 359 °C and ~ 63% (by weight) weight loss between 359 °C ~ 390 °C were observed, respectively. The thermal stability of PAM-*ran*-PMMA copolymers was obviously lower than that of PAM homopolymers [31].

Chain extension process

Chain extension reaction was conducted at 25 °C using PAM-*ran*-PMMA copolymer ($M_{n,GPC}$12100 g/mol, M_w/M_n1.42) as macroinitiator. After polymerization, the shift of the GPC peaks toward higher molecular weight region demonstrated a successful chain extension reaction. GPC analysis revealed that the $M_{n,GPC}$ of copolymers was 26,200 g/mol with M_w/M_n of 1.36, as shown in Fig. 5.

Conclusion

Well-defined PAM-*ran*-PMMAs were successfully synthesized by Cu(0)-catalyzed living radical polymerization of AM with MMA in DMF at 25 °C. The polymerization obeyed pseudo first-order kinetics, and a linear increase of M_n with monomer conversion. The polydispersity of molecular weight of copolymers was relatively narrow. By means of the Fineman–Ross equation, the comonomer reactivity ratios of AM and MMA were 0.81 and 3.21, respectively. The chain extension verified the living nature of the copolymerization. The enhanced thermal stability of PAM-*ran*-PMMA copolymers was found with the increasing of AM units in the copolymer chain.

Acknowledgements We thank the National Natural Science Foundation of China (No. 51674117, 52173279), the Provincial Natural Science Foundation of China's Hunan Province (No. 2020JJ4332), Scientific Research Fund of Hunan Provincial Education Department (No. 20A220, 20A215), the Key Laboratory of Hunan Province for Advanced Carbon-based Functional Materials, School of Chemistry and Chemical Engineering, Hunan Institute of Science and Technology, Yueyang, 414006, China, and Hunan Province (Xiangcai Construction Hunan Province, Xiangcai Construction).

References

1. NothlingMD CaoH, McKenzie TG, Hocking DM, Strugnell RA, Qiao GG (2021) Bacterial redox potential powers controlled radical polymerization. J Am Chem Soc 143:286–293
2. Azuma Y, Terashima T, Sawamoto M (2017) Self-folding polymer iron catalysts for living radical polymerization. ACS Macro Lett 6:830–835
3. OliverS ZL, Gormley AJ, Chapman R, Boyer C (2019) Living in the fast lane-high throughput controlled/living radical polymerization. Macromolecules 52:3–23
4. Dervaux B, Camp WV, Du Prez FE (2008) Amphiphilic block and "block and like" copolymers based on poly(isobornyl acrylate) and poly(acrylic acid) via ATRP. Polym Prep 49:6–7
5. Lyra EP, Petzhold CL, Lona LMF (2019) Tin(II) 2-ethylhexanoate and ascorbic acid as reducing agents in solution ARGET ATRP: a kinetic study approach by mathematical modeling and simulation. Chem Eng J 364:186–200
6. Zhou Y, Wang K, Hu D (2021) An aqueous approach to functionalize waterlogged archaeological wood followed by improved surface-initiated ARGET ATRP for maintaining dimensional stability. Cellulose 28:2433–2443
7. Min K, Gao H, Matyjaszewski K (2007) Use of ascorbic acid as reducing agent for synthesis of well-defined polymers by ARGET ATRP. Macromolecules 40:1789–1791
8. Karkare P, Kumar S, Murthy CN (2019) ARGET-ATRP using β-CD as reducing agent for the synthesis of PMMA-*b*-PS-*b*-PMMA triblock copolymers. J Appl Polym Sci 136:47117
9. Paterson SM, Brown DH, Chirila TV, Keen I, Whittaker AK, Baker MV (2010) The synthesis of water-soluble PHEMA via ARGET ATRP in protic media. J Polym Sci 48:4084–4092
10. Kwak Y, Magenau AJD, Matyjaszewski K (2011) ARGET ATRP of methyl acrylate with inexpensive ligands and ppm concentrations of catalyst. Macromolecules 44:811–819
11. Leophairatana P, Samanta S, De Silva CC, Koberstein JT (2017) Preventing alkyne-alkyne (i.e., Glaser) coupling associated with the ATRP synthesis of alkyne-functional polymers/macromonomers and for alkynes under click (i.e., CuAAC) reaction conditions. J Am Chem Soc 139:3756–3766
12. Li Z, Shi S, Fei Y, Cao D, Zhang K, Wang B, Zhe Ma, Li P, Li Y (2020) Supertough and transparent poly(lactic acid) nanostructure blends with minimal stiffness loss. ACSOmega 5:13148–13157
13. Wu X, Chen X, Shi L, Fan Z (2016) Preparation, structure and properties of PLLA-TMC/PDLA-TMC stereocomplexes. Chem J Chin Univ 37:2101–2107
14. Zhong Z, Wang X, Zhao S, Peng F, Wang J, Ying L, Yang W, Peng J, Cao Y (2017) Effects of a random copolymer's component

distribution on its opto-electronic properties. J Mater Chem C 5:6163–6168
15. Tévenot Q, Kawahara S (2021) ATRP-ARGET of a styrene monomer onto modified natural rubber latex as an initiator. Langmuir 37:6151–6157
16. Cao J, Song T, Zhu Y, Wang S, Wang X, Lv F, Jiang L, Sun M (2018) Application of amino-functionalized nanosilica in improving the thermal stability of acrylamide-based polymer for enhanced oil recovery. Energy Fuel 32:246–254
17. Teh CY, Budiman PM, Shak KPY, Wu TY (2016) Recent advancement of coagulation-flocculation and its application in wastewater treatment. Ind Eng Chem Res 55:4363–4389
18. Alsubaie FM, Alothman OY, Alshammari BA, Fouad H (2021) Facile synthesis of hydrophilic homo-polyacrylamides via Cu(0)-mediated reversible deactivation radical polymerization. Polymers 13:1947–1958
19. Fan Y, Cao H, van Mastrigt F, Pei Y, Picchioni F (2018) Copper-mediated homogeneous living radical polymerization of acrylamide with waxy potato starch-based macroinitiator. Carbohyd polym 192:61–68
20. Abdurrahmanoglu S, Can V, Okay O (2009) Design of high-toughness polyacrylamide hydrogels by hydrophobic modification. Polymer 50:5449–5455
21. Wu S, Shanks RA (2004) Synthesis and characterization of hydrophobic modified polyacrylamide. Polym Int 53:1821–1830
22. Zhou Y, Zheng H, Huang Y, Zheng X, Liu Z, An Y, Liu Y (2019) Hydrophobic modification of cationic microblocked polyacrylamide and its enhanced flocculation performance for oily wastewater treatment. J Mater Sci 54:10024–10040
23. Zhuang L, Zhi X, Du B, Yuan S (2020) Preparation of elastic and antibacterial chitosan-citric membranes with high oxygen barrier ability by in situ cross-linking. ACS Omega 5:1086–1097
24. Hsiao S-H, Wang HM (2016) Facile fabrication of redox-active and electrochromic poly(amide-amine) films through electrochemical oxidative coupling of arylamino groups. Polym Chem 54:2476–2485
25. Zhang H, Carrillo-Navarrete F, López-Mesas M, Palet C (2020) Use of chemically treated human hair wastes for the removal of heavy metal ions. Water 12:1263–1273
26. Oualid HA, Abdellaoui Y, Laabd M, Ouardi ME, Brahmi Y, Iazza M, Oualid JA (2020) Eco-efficient green seaweed codium decorticatum biosorbent for textile dyes: characterization, mechanism, recyclability, and RSM optimization. ASC Omega 5:22192–22207
27. Song YY, Dong B, Wang SW, Wang ZR, Zhang M, Tian P, Wang GC, Zhao Z (2020) Selective oxidation of propylene on $Cu_2O(111)$ and $Cu_2O(110)$ surfaces: a systematically DFT study. ACS Omega 5:6260–6269
28. Andal V, Buvaneswari G (2017) Effect of reducing agents in the conversion of Cu_2O nanocolloid to Cu nanocolloid. Eng Sci Technol 20:340–344
29. Fineman M, Ross SD (1950) Linear method for determining monomer reactivity ratios in copolymerization. J Polym Sci 5:259–262
30. Saini G, Leoni A, Franco S (1971) Solvent effects in radical copolymerization:1. Acrylamide Macromol Chem 144:235–244
31. Ryu JH, Han NK, Lee JS, Jeong YG (2019) Microstructure, thermal and mechanical properties of composite films based on carboxymethylated nanocellulose and polyacrylamide. Carbohyd Polym 211:84–90